THE JOURNAL OF BIOLOGICAL CHEMISTRY VOL. 286, NO. 11, pp. 9840–9848, March 18, 2011

Cardiac Myocyte-specific Ablation of Follistatin-like 3 Attenuates Stress-induced Myocardial Hypertrophy*[S]

Received for publication, October 22, 2010, and in revised form, December 22, 2010 Published, JBC Papers in Press, January 18, 2011, DOI 10.1074/jbc.M110.197079

Masayuki Shimano[‡1], Noriyuki Ouchi[‡], Kazuto Nakamura[‡], Yuichi Oshima[‡], Akiko Higuchi[‡], David R. Pimentel[‡], Kalyani D. Panse[§], Enrique Lara-Pezzi[‡¶], Se-Jin Lee[‖], Flora Sam[‡], and Kenneth Walsh[‡2]

From the [‡]Whitaker Cardiovascular Institute, Boston University Medical Campus, Boston, Massachusetts 02118, the [§]Heart Science Centre, Imperial College London, Hill End Road, Harefield, Middlesex UB9 6JH, United Kingdom, the [¶]Centro Nacional de Investigaciones Cardiovasculares, Melchor Fernandez Almagro 3, Madrid 28029, Spain, and the [‖]Department of Molecular Biology and Genetics, The Johns Hopkins University, Baltimore, Maryland 21205

Transforming growth factor-β family cytokines have diverse actions in the maintenance of cardiac homeostasis. Follistatin-like 3 (Fstl3) is an extracellular regulator of certain TGF-β family members, including activin A. The aim of this study was to examine the role of Fstl3 in cardiac hypertrophy. Cardiac myocyte-specific *Fstl3* knock-out (KO) mice and control mice were subjected to pressure overload induced by transverse aortic constriction (TAC). Cardiac hypertrophy was assessed by echocardiography and histological and biochemical methods. KO mice showed reduced cardiac hypertrophy, pulmonary congestion, concentric LV wall thickness, LV dilatation, and LV systolic dysfunction after TAC compared with control mice. KO mice displayed attenuated increases in cardiomyocyte cell surface area and interstitial fibrosis following pressure overload. Although activin A was similarly up-regulated in KO and control mice after TAC, a significant increase in Smad2 phosphorylation only occurred in KO mice. Knockdown of *Fstl3* in cultured cardiomyocytes inhibited PE-induced cardiac hypertrophy. Conversely, adenovirus-mediated Fstl3 overexpression blocked the inhibitory action of activin A on hypertrophy and Smad2 activation. Transduction with Smad7, a negative regulator of Smad2 signaling, blocked the antihypertrophic actions of activin A stimulation or Fstl3 ablation. These findings identify Fstl3 as a stress-induced regulator of hypertrophy that controls myocyte size via regulation of Smad signaling.

Cardiac hypertrophy is initially an adaptive response to preserve left ventricular (LV)[3] function in response stresses, but sustained hypertrophic growth of the myocardium leads to an increased risk of cardiovascular events and death (1). Therefore, a better understanding of the processes that regulate cardiac hypertrophy could lead to the development of new treatments for heart failure (2). To this end, a number of recent studies have sought to identify secreted proteins, referred to as cardiokines or cardiomyokines, that modulate cardiac hypertrophy via endocrine, paracrine, or autocrine mechanisms (3–5).

Transforming growth factor-β (TGF-β) superfamily proteins exert diverse roles in embryonic development, organ homeostasis, and the response to injury (6, 7). Activin A and myostatin, TGF-β superfamily factors, are negative regulators of tissue growth (8, 9). Recent reports indicate that activin A transcript levels are induced in congestive heart failure (10), and both activin A (11) and myostatin (12) can attenuate cardiac hypertrophy *in vitro*. Follistatin (Fst) and follistatin-like (Fstl) proteins are extracellular regulators of TGF-β superfamily members (9). Both Fst and Fstl3 bind to and antagonize the action of activin A and myostatin (13, 14), but Fstl3 binds activin A with a much higher affinity than Fst through its N-terminal domain (15). Although Fstl3 shares structural and functional homology with Fst (16), Fstl3 is preferentially expressed in heart whereas Fst is not (17). Proteins antagonized by Fstl3, (*e.g.* activin A, myostatin, and BMP2) function to promote receptor-mediated Smad signaling (14, 18, 19). Smad proteins have been implicated in the regulation of cardiac hypertrophy, including Smad2, 3, and 4 (20–23). Similarly, the TGF-β family ligand, BMP2, is reported to have a protective effect on cultured cardiac myocytes through activation of the Smad1 pathway (24).

We recently demonstrated that *Fstl3*, but not *Fst*, is up-regulated in heart in response to injuries and that it antagonized the protective role of activin A in a model of myocardial ischemia-reperfusion injury (25). In addition, *Fstl3* transcript expression is up-regulated in cardiac myocytes of patients with end-stage heart failure and associated with the severity of the disease (26). However, the possible role of Fstl3 in cardiac hypertrophy and the mechanisms underlying its effect are not understood at a molecular level. To explore the role of Fstl3 in pathological cardiac myocyte growth, we examined the effects of cardiomyocyte-specific ablation of *Fstl3* on the response to hypertrophic stimulation in mouse heart and cultured neonatal ventricular myocytes. We demonstrate that cardiac myocyte expression of Fstl3 is necessary for the full development of car-

* This work was supported, in whole or in part, by National Institutes of Health Grants AG015052, AG034972, HL068758, HL102874, and DK089875 (to K. W.) and AR060636 (to S.-J. L.).

[S] The on-line version of this article (available at http://www.jbc.org) contains supplemental Figs. 1–4.

[1] Supported by the Banyu Fellowship Program sponsored by Banyu Life Science Foundation International.

[2] To whom correspondence should be addressed: Molecular Cardiology/Whitaker Cardiovascular Institute, Boston University Medical Campus, 700 Albany St., W611, Boston, MA 02118. Tel.: 617-414-2390; Fax: 617-414-2391; E-mail: kxwalsh@bu.edu.

[3] The abbreviations used are: LV, left ventricular; ALK, activin receptor-like kinase; ANF, atrial natriuretic factor; BNP, brain natriuretic peptide; CSA, cell surface area; Fst, follistatin; Fstl, follistatin-like; NRVM, neonatal rat ventricular myocyte; PE, phenylephrine; sk-actin, skeletal-actin; Smad, Sma- and Mad-related protein; TAC, transverse aortic constriction.

diac hypertrophy through a mechanism involving, at least in part, the inhibition of stress-induced activin A/Smad2 signaling.

EXPERIMENTAL PROCEDURES

Materials—Antibodies against phosphorylated Smad2 (Ser^{465}/Ser^{467}), Smad2, phosphorylated Smad1 (Ser^{463}/Ser^{465})/Smad5 (Ser^{463}/Ser^{465}), Smad1, Smad4, Smad6, and glyceraldehyde-3-phosphate dehydrogenase (GAPDH) were purchased from Cell Signaling Technology. Dulbecco's modified Eagle's medium (DMEM) was purchased from Invitrogen. Activin A levels were determined using ELISA kits (R&D Systems).

Primary Neonatal Rat Ventricular Myocytes Culture—Primary culture of neonatal rat ventricular myocytes (NRVMs) were prepared as described previously (27). NRVMs were incubated in DMEM supplemented with 7% fetal calf serum (FCS) for 18 h after preparation and subsequently transfected with the rat small interfering RNA (siRNA) reagent, purchased from Dharmacon Inc., that represents a mixture of four different siRNAs that target *Fstl3* (SMARTpool®). Transfection was performed by Lipofectamine 2000 reagent (Invitrogen) according to the manufacturer's protocol. Forty-eight hours after transfection, NRVMs were incubated with phenylephrine (PE, 100 μmol/liter). In some experiments, NRVMs were infected with adenoviral vectors expressing Fstl3 (Ad-Fstl3), Smad7 (Ad-Smad7), Smad2 (Ad-Smad2), or β-galactosidase (Ad-β-galactosidase) at a multiplicity of infection of 50 for 8 h in DMEM. The media were then replaced with fresh DMEM without adenovirus. Forty-eight hours after infection, NRVMs were incubated with PE (100 μmol/liter). In other experiments, serum-deprived NRVMs were incubated with recombinant activin A (100 ng/ml; Sigma) for 24 h. NRVMs were also preincubated with the activin receptor-like kinase (ALK) inhibitor, SB431542 (10 μmol/liter; Calbiochem) for inhibition of Smad2 phosphorylation for 1 h prior to activin A treatment.

Transverse Aortic Constriction (TAC) Protocol—Studies using cardiac myocyte specific *Fstl3* knock-out mice (KO) in a C57BL/6 background were approved by the Institutional Animal Care and Use Committee of Boston University. As described previously (25), cardiac myocyte-specific Fstl3-deficient mice were generated by crossing $Fstl3^{flox/flox}$ with transgenic mice expressing Cre-recombinase under the control of the α-myosin heavy chain promoter (The Jackson Laboratory) (28). We compared KO mice (Cre-$Fstl3^{flox/flox}$) with control (Cre-$Fstl3^{+/+}$) mice. Mice (8–10 weeks old) were anesthetized with sodium pentobarbital (50 mg/kg intraperitoneally). The chest was opened, and the thoracic aorta was identified after blunt dissection through the intercostal muscles. A 7–0 silk suture was placed around the transverse aorta and tied around a 26-gauge blunt needle, which was subsequently removed as described previously (4). Sham-operated mice underwent a similar surgical procedure without constriction of the aorta. Animals were anesthetized and then killed. The hearts and lungs were removed and weighed. In some experiments, heart and blood samples were extracted 7 days after TAC.

Echocardiography—After 21 days, we subjected surviving mice to transthoracic echocardiography to determine cardiac function and structure. To measure LV systolic function and chamber dimensions, we performed echocardiography with an Acuson Sequoia C-256 machine using a 15-MHz probe. After we obtained a two-dimensional image, we quantified diastolic interventricular septum, diastolic posterior wall thickness, LV end diastolic diameter, and percent LV fractional shortening from M-mode images.

Histology—Mice were killed, and LV tissue was obtained 21 days after the TAC procedure. Heart samples were embedded in OCT compound (Miles) and frozen in liquid nitrogen. Tissue slices (7 μm in thickness) were prepared. To determine the myocyte cell surface area (CSA) and the levels of myocardial interstitial fibrosis, sections stained with Masson's trichrome were quantified, as described previously (4).

Western Blot Analysis—Tissue samples obtained on postoperative day 7 were homogenized in lysis buffer (Cell Signaling Technology) with protease inhibitor mixture (Sigma). Protein content was determined by the Bradford method. Equal amounts of protein (100 μg) were separated in denaturing 8–12% polyacrylamide gels and transferred to nitrocellulose membranes. Membranes were immunoblotted with primary antibodies at a 1:1,000–5,000 dilution followed by the secondary antibody conjugated with horseradish peroxidase (HRP) at a 1:1,000–10,000 dilution. Proteins were visualized using ECL Western blotting detection kit (Amersham Biosciences). To detect Fstl3 in heart, lysates were concentrated ~10-fold using a Microcon device (Millipore) prior to analysis.

RNA Isolation and Quantitative RT-PCR—Total RNA was prepared from mouse heart by using an RNA isolation kit for fibrous tissue (Qiagen). Total RNA from cultured cells was prepared with an RNA isolation kit (Qiagen). Complementary DNA (cDNA) was synthesized from 500 ng of total RNA by using SuperScript RT-PCR Systems (Invitrogen). Quantitative real-time RT-PCR was carried out on an iCycler (Bio-Rad), using SYBR Green (Applied Biosystems). The primer sequences used were as follows: mouse: *GAPDH* forward (F), 5′-TCACCACCATGGAGAAGGC-3′ and reverse (R), 5′-GCTAAGCAGTTGGTGGTGCA-3′; *Fstl3* F, 5′-CAACCCCGGCCAAGAACT-3′ and R, 5′-CTTCCTCCTCTGCTGGTACTTTG-3′; *activin A* F, 5′-TGGTGCCAGTCTAGTGCTTC-3′ and R, 5′-CCGTCACTCCCATCTTTCTT-3′; rat: *GAPDH* forward (F), 5′-TCAAGAAGGTGGTGAAGCAG-3′ and reverse (R), 5′-AGGTGGAAGAATGGGAGTTG-3′; *Fstl3* F, 5′-CGTTACCTACATCTCGTCGTGT-3′ and R, 5′-TCTCTTCCTCCTCTGCTGGTA-3′; *activin A* F, 5′-ATGTGCGGATTGCTTGTG-3′ and R, 5′-CTTCCCGTCTCCATCCA-3′. The expression levels of examined transcripts were compared with those of *GAPDH* and normalized to the mean value of controls.

Statistical Analysis—Data are presented as mean ± S.E. Group differences were analyzed by two-tailed Student's *t* test or analysis of variance (ANOVA). To compare multiple groups, the Mann-Whitney *U* test with Bonferroni correction was used. A value of $p < 0.05$ was considered statistically significant.

RESULTS

Cardiac Myocyte-specific Fstl3 Deletion Attenuates Pressure Overload-induced Cardiac Hypertrophy and Dysfunction—To investigate the role of Fstl3 in cardiac hypertrophy, α-myosin heavy chain $Cre^{+/-}$;$Fstl3^{flox/flox}$ knock-out (KO) mice were used in which *Fstl3* exons 3–5 are deleted in a cardiomyocyte-specific manner. Pressure overload cardiac hypertrophy was induced by TAC, and the mice were studied 21 days later. Following TAC, 12 of 15 WT mice and 11 of 16 KO mice survived this procedure. Although both WT and KO mice showed an increase in heart weight/body weight and lung weight/body weight ratios after banding, KO mice displayed significant reductions in these parameters (Fig. 1, *A* and *B*). No differences in these parameters were detected between control and KO mice in sham-operated mice. Likewise, no differences were detected between WT C57BL/6 mice that were either positive or negative for the Cre transgene, either at base line or following TAC, under the conditions of our assays (supplemental Fig. 1).

Echocardiographic analysis demonstrated that KO mice subjected to TAC had reduced LV wall thickness and improved LV systolic function, as indicated by smaller LV end diastolic dimension and greater percent fractional shortening compared with control mice (Fig. 1, *C–F*). Histological analysis revealed an increase in CSA of cardiac myocytes and in LV interstitial fibrosis in both control and KO mice after TAC (Fig. 1, *G–I*). However, KO mice showed significantly lower CSA and fibrosis compared with control mice. Collectively, these data show that Fstl3 is required for the full development of the hypertrophic response, whereas no significant differences in cardiac parameters were observed between the two strains under base-line conditions in the sham-operated hearts.

Analyses of Fstl3, Activin A, and Signaling in Hearts after TAC Injury—Levels of Fstl3 and activin A, a high affinity binding partner of Fstl3 (15, 18), were assessed in the sham and TAC-treated hearts. Consistent with our previous study (25), *Fstl3* and *activin A* transcript levels in the hearts of control mice were up-regulated 9- and 3-fold, respectively, 1 week after pressure overload (Fig. 2, *A* and *B*). Protein levels of Fstl3 also increased in control mice, but this induction was absent in the KO mice after TAC (Fig. 2*A*), suggesting that the induction of Fstl3 expression by hypertrophic stimuli takes place primarily in cardiac myocytes. KO mice also displayed reductions in basal *Fstl3* transcript and Fstl3 protein levels in sham hearts. Activin A transcript levels in heart and circulating protein levels increased after TAC, but no differences were found between KO and control mice (Fig. 2, *B* and *C*). Similarly, there were no differences in myostatin transcript levels in heart between the two strains (Fig. 2*D*).

To determine the effect of Fstl3 ablation on the possible participation of Smad signaling in pressure overload cardiac hypertrophy, the expression and phosphorylation of different Smad proteins at 1 week after TAC were assessed by Western blot analysis. As shown in Fig. 2*E*, the phosphorylation of Smad2 at Ser^{465}/Ser^{467} did not differ under sham-operated conditions between KO and control mice or after TAC in control mice. However, Smad2 phosphorylation was increased in response to TAC in KO mice. In contrast, no changes were detected in the myocardial expression and/or phosphorylation of Smad1/5, Smad4, or Smad6 protein either between mouse strains or in response to TAC (supplemental Fig. 2). Therefore, the effect of Fstl3 ablation appeared to specifically affect Smad2 signaling under conditions of pressure overload.

Ablation of Fstl3 Inhibits Cardiac Myocyte Growth in Vitro—To examine the role of Fstl3 in cardiac growth at a mechanistic level, an *in vitro* model of cardiac myocyte hypertrophy using PE and siRNA-mediated down-regulation of *Fstl3* expression was employed. PE treatment increased the transcript levels and protein of *Fstl3* and *activin A* in NRVMs (Fig. 3, *A–D*). Transfection of NRVMs with siRNA against *Fstl3* resulted in a 69% decrease in *Fstl3* mRNA levels under basal conditions and 79% under PE stimulation conditions (Fig. 3*A*). In contrast, Fstl3 knockdown did not alter basal or PE-induced activin A expression at the mRNA (Fig. 3*C*) or protein (Fig. 3*D*) levels, but Smad2 phosphorylation was increased in response to PE in the *Fstl3* knockdown condition (Fig. 3*E*). Knockdown of Fstl3 did not affect myocyte CSA under basal conditions, but it inhibited the PE-mediated increase in CSA (Fig. 3, *F* and *G*). The ablation of Fstl3 in cardiomyocytes markedly attenuated PE-stimulated protein synthesis as assessed by [^{3}H]leucine uptake (Fig. 3*H*). Fstl3 knockdown also inhibited PE-induced brain natriuretic peptide (BNP), atrial natriuretic factor (ANF), and α-skeletal actin (sk-actin) expression (Fig. 4).

To explore the role of Smad signaling in *Fstl3* modulation of stress-induced cardiac hypertrophy, a series of experiments were performed with an adenoviral vector expressing Smad7, an inhibitor of Smad2 activity (29). As shown in Fig. 4*A*, transduction with Smad7 reversed the inhibitory action of Fstl3 knockdown on the PE-induced increase in myocyte CSA. Consistent with these data, treatment with 10 μM SB431542, a specific inhibitor of TGF-β superfamily type I ALK receptors (ALK4, 5, and 7) (30), blocked the inhibition of PE-induced myocytes hypertrophy by *Fstl3* knockdown (Fig. 5*A*). The attenuation of PE-stimulated cardiac marker expression (ANF, BNP, and sk-actin) by *Fstl3* ablation was also reversed by transduction with Ad-Smad7 (Fig. 4, *B–D*). Similarly, treatment with SB431542 also reversed the suppressive actions of Fstl3 knockdown on PE-induced BNP, ANF, and sk-actin expression in cultured myocytes (Fig. 5, *B–D*). As shown in Figs. 4*E* and 5*E*, both SB431542 and Smad7 abolished PE-stimulated Smad2 phosphorylation. Collectively, these data suggest that Fstl3 modulates stress-induced hypertrophy via regulation of ALK-mediated Smad signaling.

Fstl3 Attenuates the Antihypertrophic Effects of Activin A—To determine whether Fstl3 overexpression has a direct effect on cardiac myocyte hypertrophy, NRVMs were transduced for 48 h with an adenoviral vector expressing Fstl3. Fstl3 overexpression, *per se*, did not alter basal or PE-stimulated myocyte CSA (supplemental Fig. 3, *A* and *B*) and had little or no effect on ANF or BNP gene expression under these conditions (supplemental Fig. 3, *C* and *D*).

Because activin A is a natural target of Fstl3, we next examined the effect of recombinant activin A on cardiomyocyte hypertrophy in the presence and absence of Fstl3 expression. As shown in Fig. 6*A*, activin A partially blocked the induction of

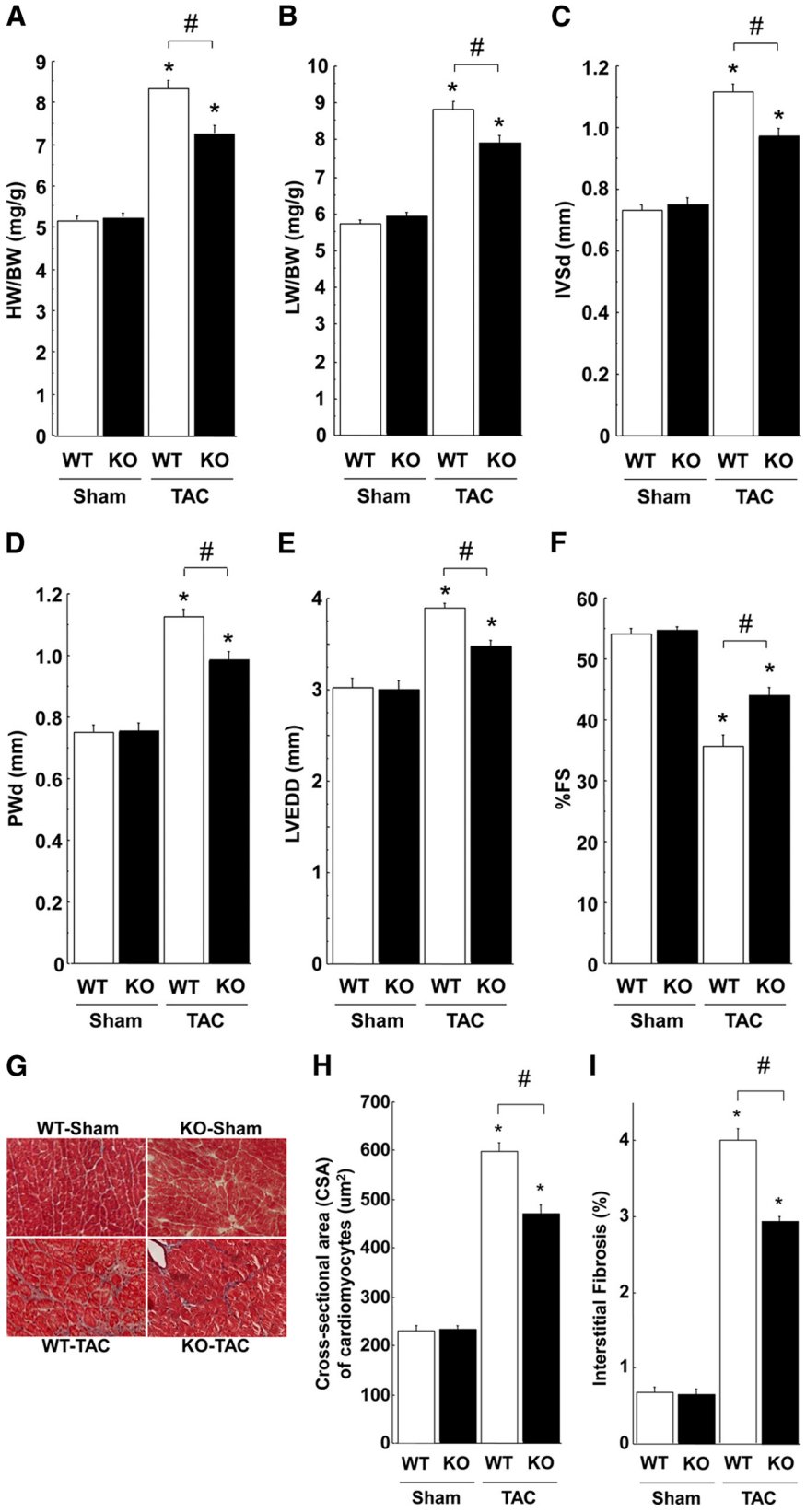

FIGURE 1. **Loss of Fstl3 attenuates exacerbation of pressure overload induced cardiac hypertrophy and heart failure.** *A* and *B*, ratio of heart weight to body weight (*HW/BW*) (*A*) and lung weight to body weight (*LW/BW*) (*B*) in WT and cardiac myocyte-specific Fstl3 mice at 3 weeks after sham operation or TAC. *C–F*, echocardiographic analysis of diastolic intraventricular septum (*IVSd*) (*C*), diastolic posterior wall (*PWd*) (*D*), LV end systolic diameter (*LVEDD*) (*E*), and the fractional shortening (*%FS*) (*F*) for WT and KO mice at 3 weeks after sham operation or TAC. *G*, representative histological LV sections from WT or KO mice stained with Masson's trichrome. Heart samples were collected at 3 weeks after sham operation or TAC. Magnification, ×400. *H* and *I*, quantitative analysis of the CSA of cardiomyocytes (*H*) and the intestinal fibrosis area (*I*) from each group. Results are presented as mean ± S.E. For sham-treated mice, $n = 6$ for WT and KO. For TAC-treated mice, $n = 12$ for WT and $n = 11$ for KO. *, $p < 0.05$ *versus* corresponding sham; #, $p < 0.05$ *versus* corresponding WT mice.

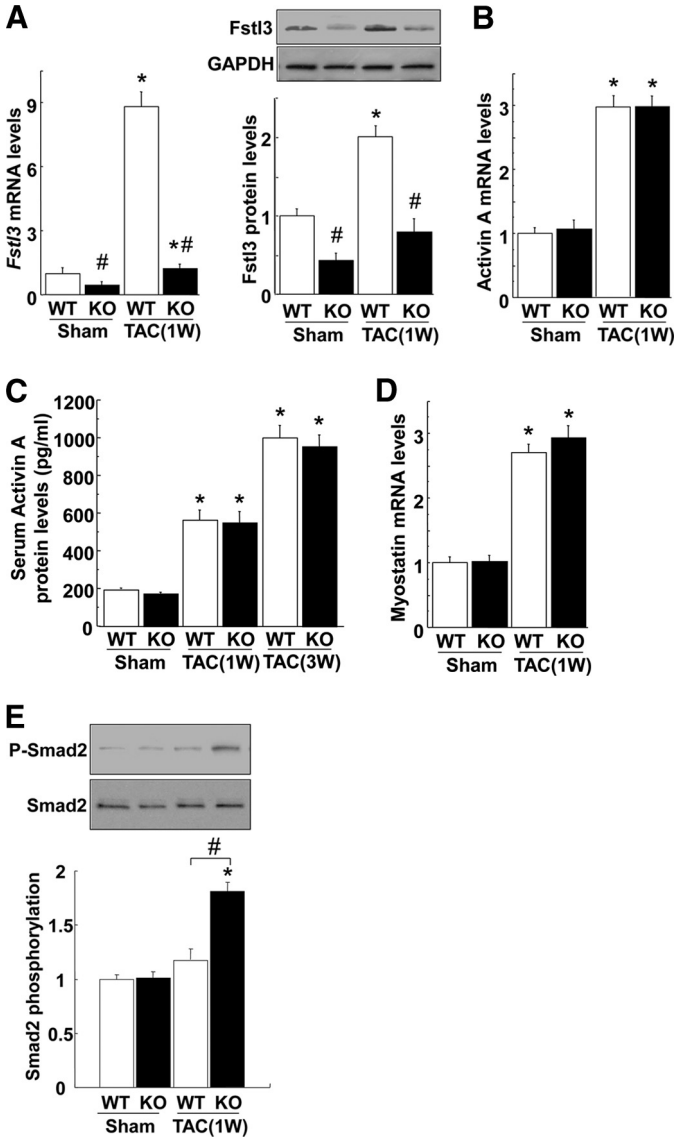

FIGURE 2. **Fstl3 deficiency leads to increased Smad2 activation following pressure overload.** *A* and *B*, Fstl3 transcript and protein levels and activin A mRNA levels in the hearts of WT and KO mice at 1 week after sham operation or TAC. *C*, serum activin A protein levels for WT and KO mice at 0, 1, or 3 weeks after TAC. *D*, myostatin mRNA levels in the hearts of WT and KO mice at 1 week after sham operation or TAC. *E*, changes in phosphorylation of Smad2 (*P-Smad2*) in the hearts of WT and KO mice at 1 week after sham operation or TAC. Representative blots of phosphorylated and total Smad2 are shown. *Lower panels* show quantitative analysis of Smad2 phosphorylation. Relative phosphorylated levels of Smad2 were normalized to control values in sham-treated WT mice ($n = 6$–12 hearts in each group). *, $p < 0.05$ *versus* corresponding sham; #, $p < 0.05$ *versus* corresponding WT mice.

cardiac hypertrophy by PE, consistent with a previous report showing that activin A inhibits leukemia inhibitory factor-induced cardiomyocyte elongation and sarcomeric organization (11). This antihypertrophic activity of activin A was neutralized by adenovirus-mediated Fstl3 overexpression. The antihypertrophic action of activin A was also suppressed by transfection with the Smad2 inhibitor, Smad7. Treatment with activin A also suppressed the PE-mediated induction of ANF, BNP, and sk-actin transcripts, and the suppressive effect of activin A on these hypertrophy markers was reversed by transduction with either Fstl3 or with Smad7 (Fig. 6, *B*–*D*). Smad2 phosphorylation by activin A was also cancelled by transduction either with Fstl3 or with Smad7 (Fig. 6*E*). Similar to stimulation with activin A, or Fstl3 ablation, expression of Smad2 diminished PE-mediated myocyte hypertrophy but had no effect on basal myocyte size (supplemental Fig. 4). The levels of Fstl3 and Smad7 overexpression in these assays can be seen in Fig. 6*F*.

DISCUSSION

The balance between members of the TGF-β superfamily (TGF-β, BMPs, activin, and myostatin) and their inhibitors (inhibins, follistatins, nodal) regulates a variety of physiological and pathological processes, including cell proliferation, differentiation, and wound healing (9). We and others have recently described that the expression of activin A and Fstl3 is induced in response to permanent left anterior descending artery ligation, myocardial ischemia-reperfusion injury, pressure-overload cardiac hypertrophy, and in end-stage heart failure patients, whereas the expression of other members of the activin/inhibin system, such as inhibin α or Fst, is not affected (25, 26, 31). The consistent increase of in Fstl3 and activin A expression in these diverse models of myocardial injury suggests that these proteins are cardiokines whose levels of expression could influence cardiac disease outcome.

Here, we show that cardiac myocyte-specific Fstl3 deficiency attenuates myocardial hypertrophy, systolic dysfunction, and LV interstitial fibrosis following pressure overload. These effects were accompanied by an increase in Smad2 phosphorylation in the heart. Given the lack of differences between control and KO mice in the absence of cardiac injury, it appears that basal levels of cardiomyocyte-derived Fstl3 expression have little or no role in cardiac homeostasis. On the contrary, Fstl3 contributes to the development of the hypertrophic response to pathological stimuli. This response is recapitulated in cultured cardiomyocytes where knockdown of Fstl3 inhibits PE-induced hypertrophy but has no effect on cell growth under basal conditions. In contrast to the findings reported here, Mukherjee *et al.* have shown that whole body Fstl3-deficient mice display no modifications of muscle nor body weight but an increase in heart size under basal conditions (32). We attribute the differences in cardiac phenotypes between the global and myocyte-specific knockouts to a consequence of the metabolic phenotypes that are associated with whole body Fstl3 ablation.

Fstl3 potentially exerts its anti-hypertrophic actions by interfering with activin A action (Fig. 5*E*). Like Fstl3, TAC leads to an increase in activin A expression in heart and in the serum. In cultured myocytes, activin A inhibits PE-induced myocyte growth and diminishes the expression of hypertrophic markers including BNP, ANF, and sk-actin. These findings are consistent with the study of Florholmen *et al.* showing that activin A inhibits the hypertrophic action of leukemia inhibitory factor (11). Here, it is shown that Fstl3 antagonizes the antihypertrophic actions of activin A on growth of myocytes that are subjected to adrenergic stimulation. Based upon chemical inhibitor studies, it has been proposed that the signaling actions of activin A are mediated by serine/threonine kinase activin type II receptors that form a heterodimeric complex with ALK4, 5, and/or 7 (33, 34). Consistent with this hypothesis, we show that

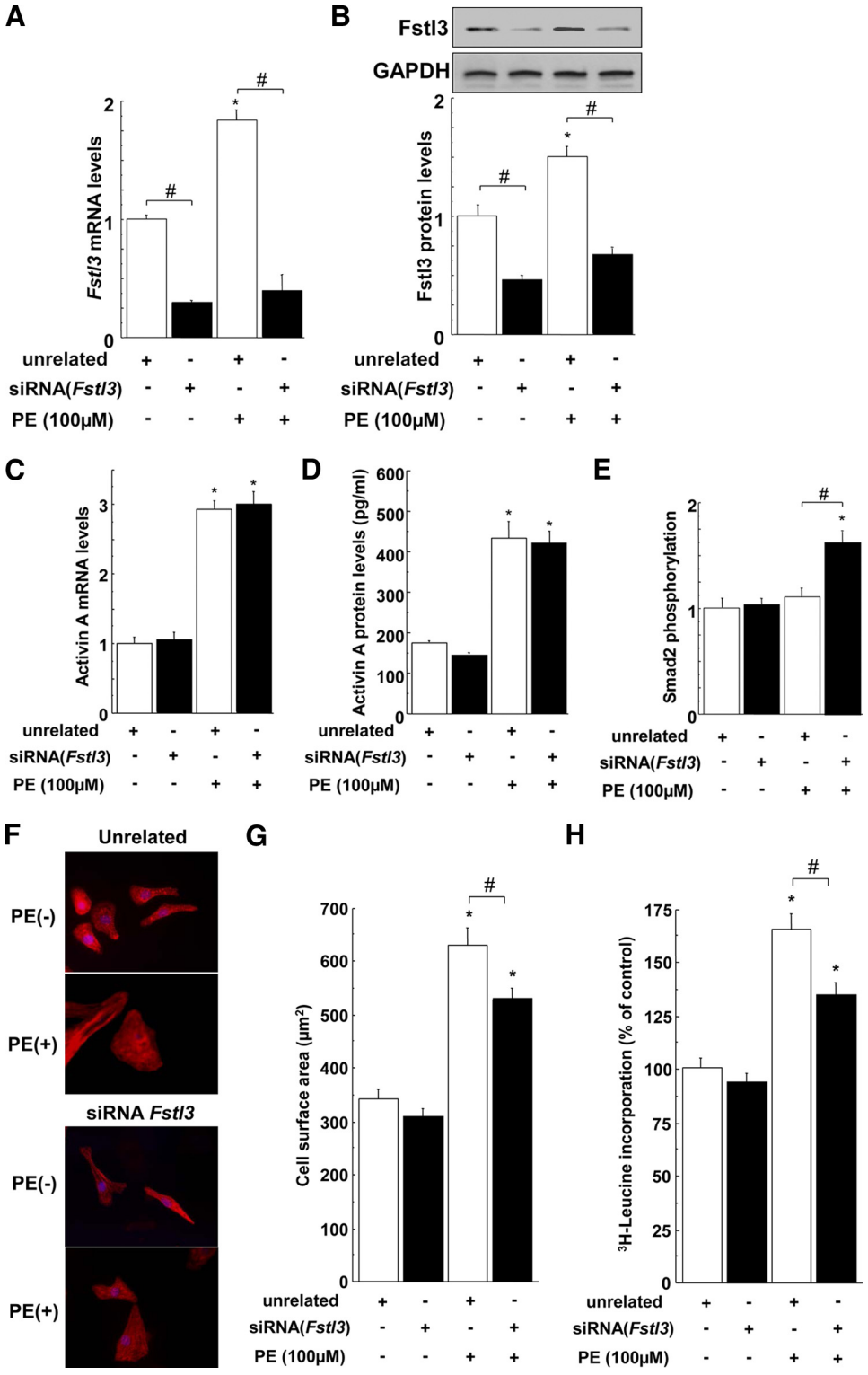

FIGURE 3. **Fstl3 ablation attenuates the hypertrophic actions of PE treatment in cultured cardiac myocytes.** *A* and *B*, results of real-time PCR and Western blot analysis of *Fstl3* (*A*) and activin A (*B*) gene expression with unrelated or *Fstl3* siRNA in the presence or absence of PE (100 μmol/liter) for 24 h. *C* and *D*, no effect of *Fstl3* deletion on activin A mRNA and protein expression by NRVMs. Activin A protein levels in media were assessed by ELISA. *E*, effect of Fstl3 knockdown on Smad2 phosphorylation. Relative phosphorylated levels of Smad2 were normalized to control values in NRVMs that were not targeted with siRNA. *F*, representative fluorescence microscope images of NRVMs transfected with unrelated siRNA or *Fstl3* siRNA for 48 h following by stimulation with phenylephrine (PE, 100 μmol/liter) for 24 h. *G* and *H*, quantitative analysis of cell surface area (*G*) and protein synthesis (*H*) assessed by [^{3}H]leucine incorporation after siRNA transfection with or without PE. *, $p < 0.05$ *versus* corresponding control without PE; #, $p < 0.05$ *versus* corresponding no-targeting siRNA.

the inhibition of ALK signaling blocks the antihypertrophic actions of either Fstl3 knockdown or activin A overexpression in cultured cardiac myocytes.

It is established that activation of ALK4, 5, or 7 receptors by activin A leads to Smad2 phosphorylation (6). Previously, it has been shown that overexpression of Smad2 in cardiomyocytes

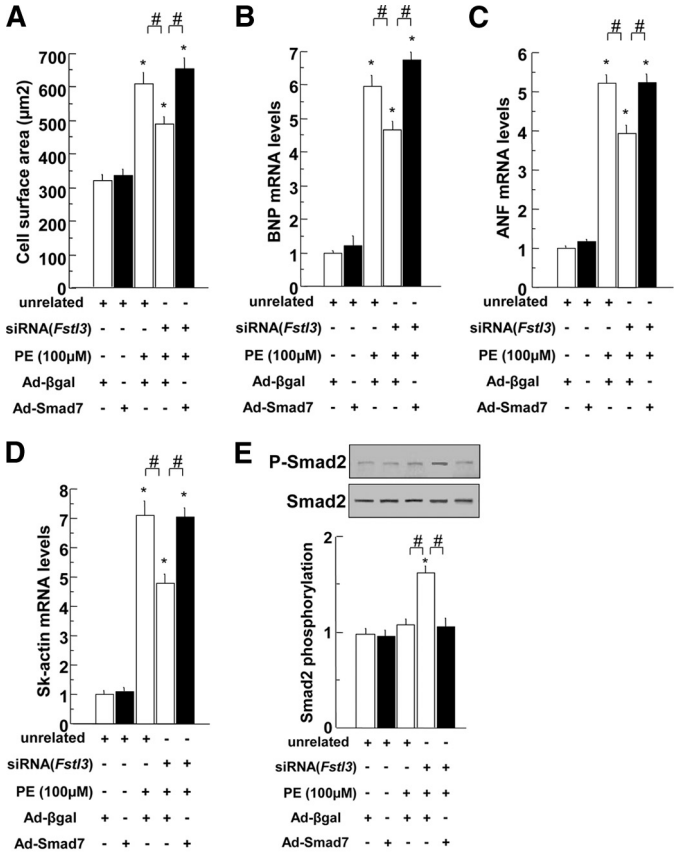

FIGURE 4. **Antihypertrophic effects of *Fstl3* knockdown are reversed by Smad7 transduction in cultured cardiac myocytes.** *A*, quantitative analysis of cell surface area after siRNA and/or Ad-Smad7 transfection with or without PE. *B–D*, results of real-time PCR analysis of BNP (*B*), ANF (*C*), and sk-actin (*D*) expression following transduction of unrelated or *Fstl3* siRNA in the presence or absence of Ad-Smad7 transduction. Some cells were treated with PE. Results are presented as mean ± S.E. ($n = 8$ per group). *E*, effect on Smad2 phosphorylation. Representative blots of phosphorylated and total Smad2 are shown. *Lower panels* show quantitative analysis of Smad2 phosphorylation. Relative phosphorylated levels of Smad2 were normalized to control values. *, $p < 0.05$ *versus* corresponding WT (both no-targeting siRNA and Ad-β-galactosidase (*Ad-βgal*)) without PE. #, statistical difference ($p < 0.05$) between indicated *bars*.

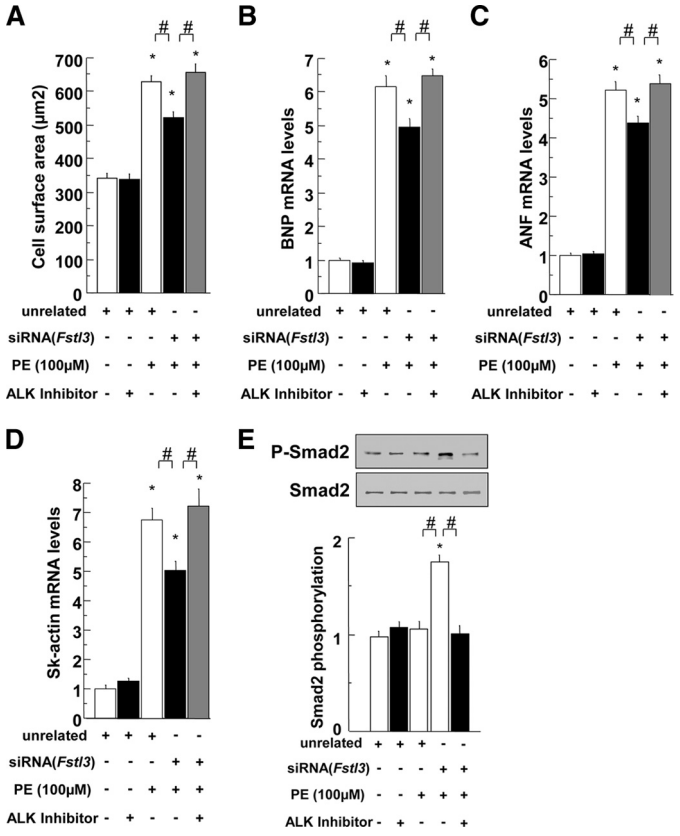

FIGURE 5. **Antihypertrophic effect of *Fstl3* knockdown can be reversed by ALK inhibition in cultured cardiac myocytes.** *A*, quantitative analysis of cell surface area after siRNA transfection with or without PE or SB432541(10 μmol/liter). *B–D*, results of quantitative RT-PCR analysis of BNP (*B*), ANF (*C*), and sk-actin (*D*) expression in NRVMs treated with unrelated or *Fstl3* siRNA in the presence or absence of PE or SB432541. *E*, effect on Smad2 phosphorylation. Representative blots of phosphorylated and total Smad2 are shown. *Lower panels* show quantitative analysis of Smad2 phosphorylation. Relative phosphorylated levels of Smad2 were normalized to control values. *, $p < 0.05$ *versus* corresponding WT without PE. #, statistical difference ($p < 0.05$) between indicated *bars*.

results in reduced hypertrophy induced by phenylephrine and angiotensin II (20). The cellular action of Smad2 is potentiated by Smad4 (35), and the myocyte-specific ablation of Smad4 in heart leads to cardiac hypertrophy (20, 21). In contrast, Smad7, an inhibitory Smad protein (29), reverses the antihypertrophic action of Smad2 in myocytes (22). Here, it is shown that myocyte-specific ablation of Fstl3 in the heart leads to the up-regulation of Smad2 phosphorylation under pressure overload, but not base-line, conditions. In contrast, these conditions did not alter the phosphorylation states of Smad1/5, nor the expression of Smad4 and Smad6. In cultured myocytes, the transduction of Smad7 functioned in a manner similar to the overexpression of Fstl3 in that both proteins reversed the antihypertrophic actions of activin A. Similarly, Smad7 reversed the antihypertrophic effect of Fstl3 knockdown.

It is noteworthy that whereas hypertrophic stimuli induce activin A expression, this is associated with increased Smad2 phosphorylation in hearts of *Fstl3* KO but not WT mice. Thus, it appears that this system is held in check because both Fstl3 and activin A are induced by hypertrophic stimuli in WT mice. However, in the Fstl3-null heart, this system of checks and balances is perturbed, and Smad2 activation becomes more prominent leading to a reduction in the hypertrophic response. Collectively, our results *in vitro* and *in vivo* suggest that activin A and Fstl3 act as a molecular rheostat to control heart growth in response to injury (Fig. 6*G*).

The mechanism underlying the prohypertrophic effect of Fstl3 appears to involve the sequestration and inactivation of TGF-β superfamily members, such as activin A, and prevention of Smad2 activation by these family members. As shown here and elsewhere, activin A is regulated by cardiac stress in murine, rattus, canine, and human systems (10, 25, 31). However, it is conceivable that Fstl3 also interacts with other TGF-β superfamily members to influence cardiac biology. For example, Fstl3 can bind to both BMP2 and myostatin which have been implicated in the control of myocyte hypertrophy and survival and myocyte communication with skeletal muscle (12, 24, 36). In this regard, other TGF-β superfamily members have been identified in the heart, and they may interact with the Fstl3/activin A/ALK regulatory system. For example, GDF-15 has been shown to exert an inhibitory effect on myocyte growth via an activation of Smad2

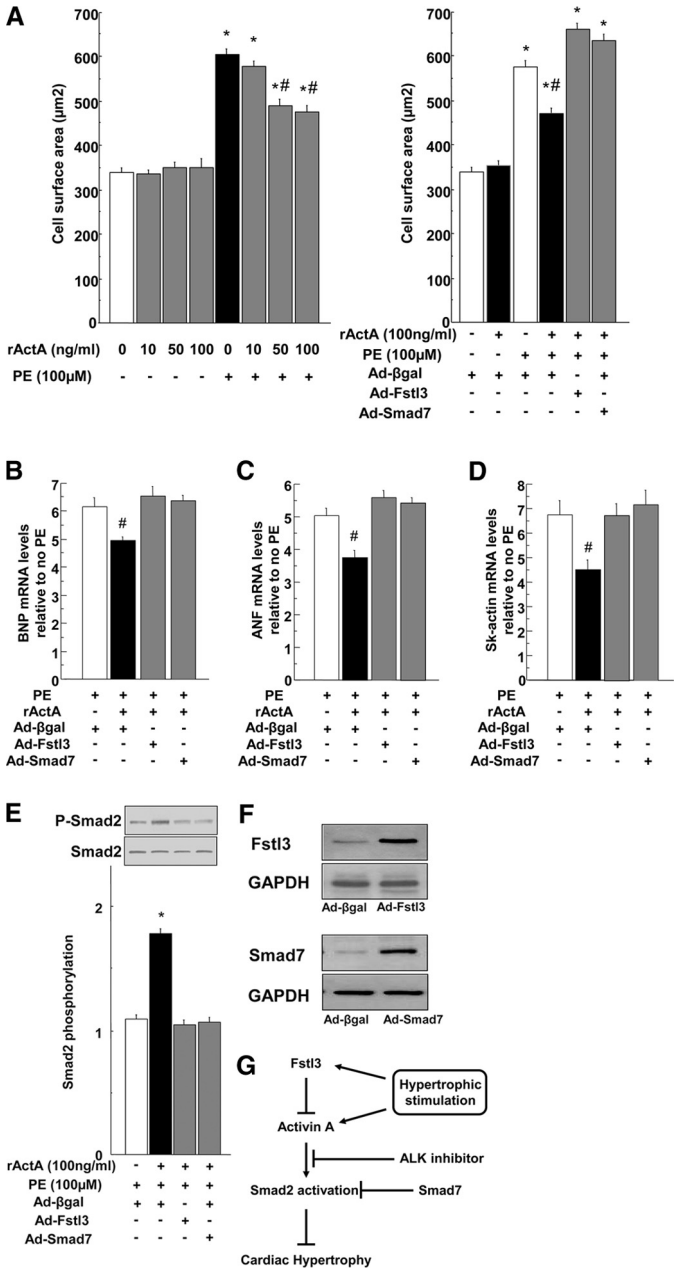

FIGURE 6. **Fstl3 impairs activin A-mediated suppression of PE-induced cardiac hypertrophy in cultured cardiac myocytes.** *A*, quantitative analysis of cell surface area after treatment with recombinant activin A protein (rActA, indicated dose or 100 ng/ml) with or without PE (100 μmol/liter) treatment. NRVMs were transfected with Ad-Fstl3, Ad-Smad7, or Ad-β-galactosidase (*Ad-βgal*). *B–D*, results of real-time PCR analysis of ANF (*B*), BNP (*C*), and sk-actin (*D*). *E*, effect on Smad2 phosphorylation. Representative blots of phosphorylated and total Smad2 are shown. *Lower panels* show quantitative analysis of Smad2 phosphorylation. Relative phosphorylated levels of Smad2 were normalized to control values. Cells were transduced with Ad-Fstl3 or Ad-Smad7 in the presence of PE inhibited to examine the regulatory activity of rActA. #, $p < 0.05$ *versus* corresponding Ad-β-galactosidase with rActA-treated cells. *F*, Western blot analysis revealed Fstl3 or Smad7 protein expression after transfection with Ad-*Fstl3* or Ad-Smad7. *G*, model of Fstl3/Activin A-mediated regulation of cardiac hypertrophy.

(22), but this factor has no known extracellular regulatory partner or cell surface receptor. Thus, further investigations of these classes of molecules in the heart could lead to the identification of new molecular targets useful for the diagnosis or treatment of cardiac disease.

Acknowledgments—We thank Drs. Aristidis Moustakas and Jeffery Molkentin for some of the adenovirus reagents used in this study.

REFERENCES

1. Levy, D., Garrison, R. J., Savage, D. D., Kannel, W. B., and Castelli, W. P. (1990) *N. Engl. J. Med.* **322,** 1561–1566
2. Molkentin, J. D., and Dorn, G. W., 2nd (2001) *Annu. Rev. Physiol.* **63,** 391–426
3. Frost, R. J., and Engelhardt, S. (2007) *Circulation* **116,** 1768–1775
4. Shibata, R., Ouchi, N., Ito, M., Kihara, S., Shiojima, I., Pimentel, D. R., Kumada, M., Sato, K., Schiekofer, S., Ohashi, K., Funahashi, T., Colucci, W. S., and Walsh, K. (2004) *Nat. Med.* **10,** 1384–1389
5. Shiojima, I., Sato, K., Izumiya, Y., Schiekofer, S., Ito, M., Liao, R., Colucci, W. S., and Walsh, K. (2005) *J. Clin. Invest.* **115,** 2108–2118
6. Shi, Y., and Massagué, J. (2003) *Cell* **113,** 685–700
7. Bujak, M., and Frangogiannis, N. G. (2007) *Cardiovasc. Res.* **74,** 184–195
8. McPherron, A. C., Lawler, A. M., and Lee, S. J. (1997) *Nature* **387,** 83–90
9. Welt, C., Sidis, Y., Keutmann, H., and Schneyer, A. (2002) *Exp. Biol. Med.* **227,** 724–752
10. Mahmoudabady, M., Mathieu, M., Dewachter, L., Hadad, I., Ray, L., Jespers, P., Brimioulle, S., Naeije, R., and McEntee, K. (2008) *J. Card. Fail.* **14,** 703–709
11. Florholmen, G., Halvorsen, B., Beraki, K., Lyberg, T., Sagen, E. L., Aukrust, P., Christensen, G., and Yndestad, A. (2006) *J. Mol. Cell. Cardiol.* **41,** 689–697
12. Morissette, M. R., Cook, S. A., Foo, S., McKoy, G., Ashida, N., Novikov, M., Scherrer-Crosbie, M., Li, L., Matsui, T., Brooks, G., and Rosenzweig, A. (2006) *Circ. Res.* **99,** 15–24
13. Schneyer, A., Sidis, Y., Xia, Y., Saito, S., del Re, E., Lin, H. Y., and Keutmann, H. (2004) *Mol. Cell. Endocrinol.* **225,** 25–28
14. Sidis, Y., Mukherjee, A., Keutmann, H., Delbaere, A., Sadatsuki, M., and Schneyer, A. (2006) *Endocrinology* **147,** 3586–3597
15. Stamler, R., Keutmann, H. T., Sidis, Y., Kattamuri, C., Schneyer, A., and Thompson, T. B. (2008) *J. Biol. Chem.* **283,** 32831–32838
16. Hayette, S., Gadoux, M., Martel, S., Bertrand, S., Tigaud, I., Magaud, J. P., and Rimokh, R. (1998) *Oncogene* **16,** 2949–2954
17. Tortoriello, D. V., Sidis, Y., Holtzman, D. A., Holmes, W. E., and Schneyer, A. L. (2001) *Endocrinology* **142,** 3426–3434
18. Tsuchida, K., Arai, K. Y., Kuramoto, Y., Yamakawa, N., Hasegawa, Y., and Sugino, H. (2000) *J. Biol. Chem.* **275,** 40788–40796
19. Hill, J. J., Davies, M. V., Pearson, A. A., Wang, J. H., Hewick, R. M., Wolfman, N. M., and Qiu, Y. (2002) *J. Biol. Chem.* **277,** 40735–40741
20. Heger, J., Peters, S. C., Piper, H. M., and Euler, G. (2009) *J. Cell. Physiol.* **220,** 515–523
21. Wang, J., Xu, N., Feng, X., Hou, N., Zhang, J., Cheng, X., Chen, Y., Zhang, Y., and Yang, X. (2005) *Circ. Res.* **97,** 821–828
22. Xu, J., Kimball, T. R., Lorenz, J. N., Brown, D. A., Bauskin, A. R., Klevitsky, R., Hewett, T. E., Breit, S. N., and Molkentin, J. D. (2006) *Circ. Res.* **98,** 342–350
23. Divakaran, V., Adrogue, J., Ishiyama, M., Entman, M. L., Haudek, S., Sivasubramanian, N., and Mann, D. L. (2009) *Circ. Heart Fail.* **2,** 633–642
24. Izumi, M., Fujio, Y., Kunisada, K., Negoro, S., Tone, E., Funamoto, M., Osugi, T., Oshima, Y., Nakaoka, Y., Kishimoto, T., Yamauchi-Takihara, K., and Hirota, H. (2001) *J. Biol. Chem.* **276,** 31133–31141
25. Oshima, Y., Ouchi, N., Shimano, M., Pimentel, D. R., Papanicolaou, K. N., Panse, K. D., Tsuchida, K., Lara-Pezzi, E., Lee, S. J., and Walsh, K. (2009) *Circulation* **120,** 1606–1615
26. Lara-Pezzi, E., Felkin, L. E., Birks, E. J., Sarathchandra, P., Panse, K. D., George, R., Hall, J. L., Yacoub, M. H., Rosenthal, N., and Barton, P. J. (2008) *Endocrinology* **149,** 5822–5827
27. Pimentel, D. R., Amin, J. K., Xiao, L., Miller, T., Viereck, J., Oliver-Krasinski, J., Baliga, R., Wang, J., Siwik, D. A., Singh, K., Pagano, P., Colucci, W. S., and Sawyer, D. B. (2001) *Circ. Res.* **89,** 453–460
28. Agah, R., Frenkel, P. A., French, B. A., Michael, L. H., Overbeek, P. A., and Schneider, M. D. (1997) *J. Clin. Invest.* **100,** 169–179

29. Nakao, A., Afrakhte, M., Morén, A., Nakayama, T., Christian, J. L., Heuchel, R., Itoh, S., Kawabata, M., Heldin, N. E., Heldin, C. H., and ten Dijke, P. (1997) *Nature* **389,** 631–635
30. Inman, G. J., Nicolás, F. J., Callahan, J. F., Harling, J. D., Gaster, L. M., Reith, A. D., Laping, N. J., and Hill, C. S. (2002) *Mol. Pharmacol.* **62,** 65–74
31. Yndestad, A., Ueland, T., Øie, E., Florholmen, G., Halvorsen, B., Attramadal, H., Simonsen, S., Frøland, S. S., Gullestad, L., Christensen, G., Damås, J. K., and Aukrust, P. (2004) *Circulation* **109,** 1379–1385
32. Mukherjee, A., Sidis, Y., Mahan, A., Raher, M. J., Xia, Y., Rosen, E. D., Bloch, K. D., Thomas, M. K., and Schneyer, A. L. (2007) *Proc. Natl. Acad. Sci. U.S.A.* **104,** 1348–1353
33. Attisano, L., Wrana, J. L., Montalvo, E., and Massagué, J. (1996) *Mol. Cell. Biol.* **16,** 1066–1073
34. Chen, Y. G., Wang, Q., Lin, S. L., Chang, C. D., Chuang, J., and Ying, S. Y. (2006) *Exp. Biol. Med.* **231,** 534–544
35. Attisano, L., and Wrana, J. L. (2002) *Science* **296,** 1646–1647
36. Heineke, J., Auger-Messier, M., Xu, J., Sargent, M., York, A., Welle, S., and Molkentin, J. D. (2010) *Circulation* **121,** 419–425